Industrial Chemistry & Materials

ROYAL SOCIETY OF CHEMISTRY

PAPER

View Article Online
View Journal | View Issue

Cite this: *Ind. Chem. Mater.*, 2023, **1**, 516

The effect of grafted alkyl side chains on the properties of poly(terphenyl piperidinium) based high temperature proton exchange membranes†

Xuefu Che,‡ Lele Wang,‡ Ting Wang, Jianhao Dong and Jingshuai Yang *

High temperature proton exchange membrane fuel cells (HT-PEMFCs) operating at elevated temperatures above 120 °C take advantage of feasible anode fuels and simplified water/heat management. A high temperature polymer electrolyte membrane (HT-PEM) is the core material for HT-PEMFCs. In this work, a series of phosphoric acid (PA) doped HT-PEMs based on poly(terphenyl piperidine) (PTP) tailored with alkyl groups are synthesized. Five different pendant alkyl groups (including methyl, propyl, pentyl, heptyl and decyl) are grafted onto the piperidine group through the Menshutkin reaction between PTP and alkyl halides. Compared with PTP and methyl grafted PTP (PTP-C1) membranes, the PTP-C*x* membranes with long alkyl side chains exhibit improved PA doping contents and conductivities. The optimized pentyl-substituted PTP membrane (PTP-C5) possessed a reasonable PA doping content (202% after immersing in 85 wt% PA at 60 °C), high proton conductivity (96 mS cm^{-1} at 180 °C) and good tensile strength (4.6 MPa at room temperature). A H_2–air single cell equipped with PTP-C5/PA consequently achieved a high peak power density of 676 mW cm^{-2} at 210 °C without any humidification or backpressure. Thus, this work provides a simple method for preparing high-performance HT-PEMs.

Received 14th June 2023,
Accepted 13th August 2023

DOI: 10.1039/d3im00064h

rsc.li/icm

Keywords: High temperature polymer electrolyte membrane; Fuel cell; Grafted membrane.

1 Introduction

The proton exchange membrane fuel cell (PEMFC) is considered as one of the most promising energy conversion systems, and has wide application prospect because of its high economic–social benefit and excellent green environmental protection advantage.[1] As one of the critical components of PEMFCs, proton exchange membranes (PEMs) play an irreplaceable role in transferring protons and isolating gases. To date, both commercial perfluorosulfonic acid membranes (*i.e.* Nafion)[2] and other pendant sulfonate group grafted polymer membranes[3,4] have shown excellent fuel cell performance under full humidification below 80 °C. However, the relatively low working temperature of PEMFCs gives rise to technical issues such as low resistance to CO poisoning, complex hydrothermal management and low electrode dynamics.[1,5] Meanwhile, the Nafion series membranes also have high production cost due to their complex synthesis and manufacturing. Consequently, it is of great significance to develop non-fluorinated high temperature proton exchange membranes (HT-PEMs) which enable fuel cells to have an operation temperature between 100 °C and 200 °C to overcome the disadvantages of Nafion based PEMFCs.[6,7]

As the core element of high temperature PEMFCs (HT-PEMFCs), HT-PEMs not only maintain excellent proton conductivities independent of water, but also possess suitable mechanical stability at elevated temperatures,[6,8] The basic polymer membranes doped with nonvolatile inorganic acid (*i.e.* phosphoric acid (PA)) have been developed for HT-PEMs.[8,9] Wainright *et al.*[10] firstly proposed the PA doped polybenzimidazole (PBI) membrane, which is now regarded as the most suitable HT-PEM for commercialization because of its excellent performance under anhydrous conditions.[6,8,11,12] Subsequently, PBI modifications and derivatives have been developed.[9,13,14] However, the carcinogenicity of the 3,3′,4,4′-tetraaminobiphenyl monomer and limited solubility of PBI in polar solvents hinder the further development of PBI membranes. Thus, the design and fabrication of new HT-PEMs with good thermal stability, modest mechanical properties and excellent proton conductivity have been encouraged.[5,8,15] Alternatively, a variety of potential candidate polymer materials with side-chain or main-chain

Department of Chemistry, College of Sciences, Northeastern University, Shenyang 110819, China. E-mail: yjs@mail.neu.edu.cn

† Electronic supplementary information (ESI) available. See DOI: https://doi.org/10.1039/d3im00064h

‡ These authors contributed equally to this work.

basic groups have been designed and realized. For example, aromatic polymer materials containing pyridine[16] and quinolone[17] have been synthesized, and pyrrolidone[18,19] and imine[20,21] containing polyolefins have been selected as HT-PEMs as well. Recently, inspired by the synthesis of wholly aromatic polymers by Zolotukhin *et al.*[22] and Tröger base (TB) containing polymers by McKeown *et al.*,[23] we successfully synthesized ether free polymers containing pendant pyridine[24,25] and a TB (*i.e.*, 1,5-methano-1,5-diazocine)[26] unit through one-step superacid catalyzed polymerization. Both the above membranes displayed considerable organic solubility, excellent chemical stability and remarkable PA doping capability, resulting in high fuel cell performance.

In addition, great efforts have been recently made on the synthesis of poly(arylene piperidine) (PAP) series membranes for various energy conversion and storage devices. For example, Jannasch *et al.* synthesized poly(arylene piperidinium) based anion exchange membranes (AEMs) through acid-catalyzed Friedel–Crafts polyhydroxyalkylation and alkyl side-chain grafting.[27] Meanwhile, Yan *et al.*[28] and Zhuang *et al.*[29] respectively assembled AEMFCs with CH_3I quaternized PAP AEMs, which achieved a significantly high peak power density above 1.0 W cm^{-2}. The presence of piperidine groups inspired researchers to prepare HT-PEMs using PAPs.[30] However, the widely used poly(*p*-terphenyl-*N*-methylpiperidine) (PTP) displayed limited solubility in normal polar solvents and moderate PA doping content.[27] In our recent work, bulky basic side chains (*e.g.* methylene benzimidazole)[31] and long side-chain ionic liquids (*e.g.* trimethylammonium pentyl[32,33] and pentyl methylimidazolium (PMIm)[34]) were introduced into PTP to enhance the PA absorption content and conductivity. These membranes displayed high performance in HT-PEMFCs and vanadium redox flow batteries. For example, without backpressure, the fuel cell based on PTP-PMIm/323% PA

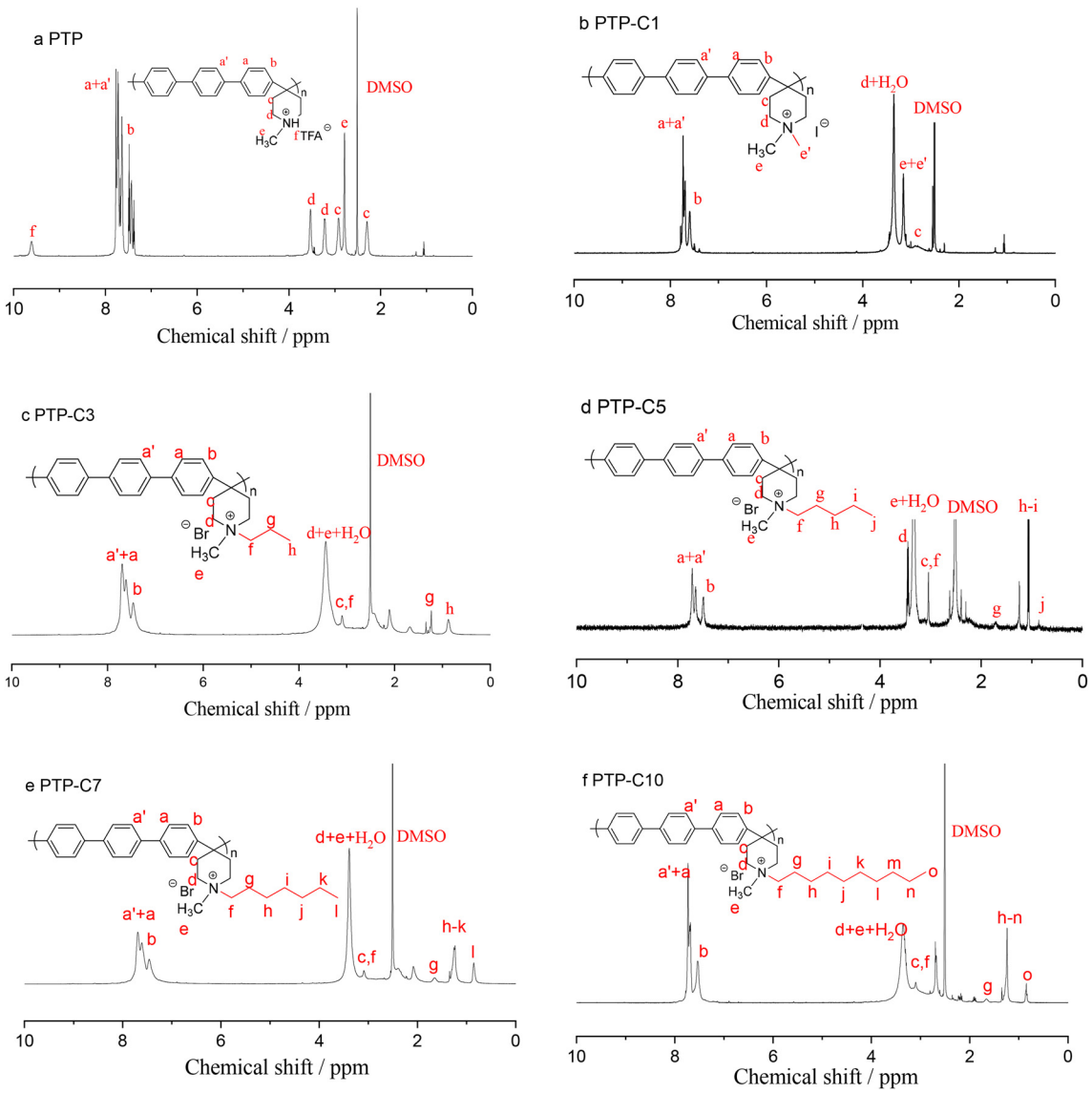

Fig. 1 ^{1}H NMR spectra of PTP (a) and various PTP-C*x* polymers (b–f).

displayed a high peak power density of 456 mW cm^{-2} at 200 °C under H_2 and air conditions.[34]

In this study, we extended our work to realizing membranes of poly(terphenyl piperidinium) tailored with alkyl groups. Five different pendant alkyl groups (including methyl, propyl, pentyl, heptyl and decyl) were grafted onto piperidinium cations through the Menshutkin reaction between PTP and alkyl halides. Accordingly, the influence of the alkyl side-chain length on the properties of quaternized PTP membranes was investigated. The optimized pentyl-substituted PTP membrane possessed reasonable PA doping content, high proton conductivity and good tensile strength. More importantly, a HT-PEMFC based on the above membrane displayed a remarkable power density.

2 Results and discussion

2.1 Synthesis of the PTP-C*x* membranes

Herein, the rigid ether-free aryl polymer of PTP was synthesized and employed as the matrix of HT-PEMs. It was found that the pure PTP polymer showed a limited solubility in common polar solvents (*e.g.* DMSO, NMP, DMF and DMAc), which possibly resulted from its rigid molecular chain as previously reported by Olsson *et al.*[27] In contrast, TFA protonated or alkyl grafted PTP exhibited good solubility in the abovementioned solvents. As a result, the viscosity and ^{1}H NMR spectrum of PTP in protonated form were determined in NMP. The viscosity of PTP reached 0.86 dL g^{-1}. Fig. 1a shows the ^{1}H NMR results for PTP. The characteristic peaks from 7.0 to 8.0 ppm ($H_{a+a',b}$) resulted from the phenyl linkages in PTP, while the characteristic peaks from 2.0 to 4.0 ppm were due to the piperidine ($H_{c,d}$) and methyl (H_e) groups.[28,30,31] Additionally, the peak at 9.6 ppm (H_f) belonged to the NH^+ group, which was produced by protonating piperidine with TFA.

In order to optimize the polymer structure and improve the membrane performance, five different pendant alkyl side chains were grafted into the piperidinium groups. The pendant alkyl side chains could adjust the hydrophilicity and the steric hindrance of the piperidinium cations and the free volume of the polymer, correspondingly affecting the

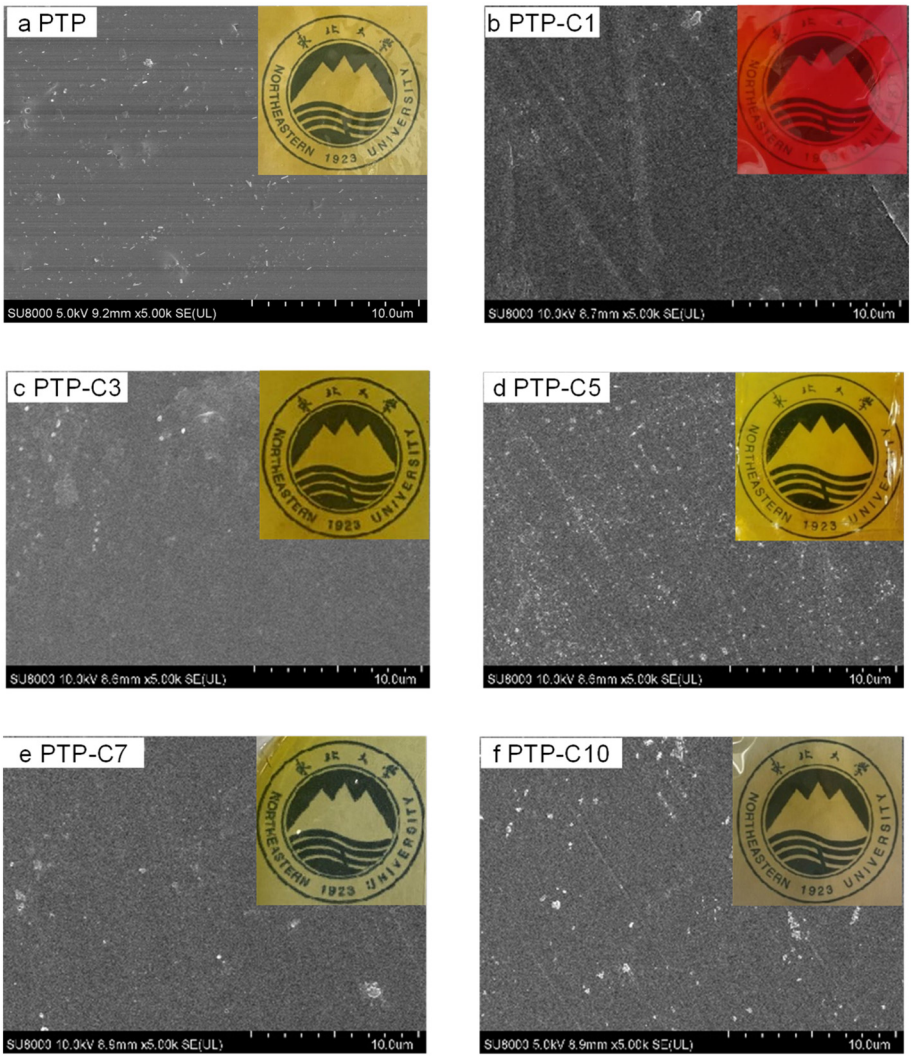

Fig. 2 Surface SEM and photographic images of the (a) PTP and (b–f) PTP-C*x* membranes.

interaction between the PA molecules and PTP polymer. Fig. 1b–f depict the ^{1}H NMR spectra of the various PTP-C*x* polymers. After grafting different alkyl side chains into the PTP backbone, new additional peaks originating from end-group methyl and methylene linkages were observed in the ^{1}H NMR spectra. As an example, for PTP-C3, the characteristic peak from the end-group methyl appeared at 0.87 ppm, while the methylene spacers in the side chain displayed characteristic peaks ranging from 1.0 to 2.5 ppm.[27,35] The characteristic peaks of the other PTP-C*x* polymers are assigned in Fig. 1 accordingly. Meanwhile, the grafting degrees (GD%) of the various PTP-C*x* polymers were determined from the integral area ratio of the characteristic peak of side-chain end-group $-CH_3$ on piperidinium cations to the characteristic peaks of aromatic phenyl groups. As the molar ratio of each alkyl halide to the PTP polymer was 1 : 1 and the quaternization reaction was carried out under the same conditions, the GD% values of PTP-C1, PTP-C3, PTP-C5, PTP-C7 and PTP-C10 were 35%, 36%, 43%, 44% and 24%, respectively. As a result, the NMR spectra prove the successful synthesis of PTP-C*x* polymers with different alkyl side chains.

Fig. 2 presents the surface SEM and photographic images of the PTP and PTP-C*x* membranes. Compared with the pristine PTP polymer, the alkyl side chain grafted PTP polymers of PTP-C*x* exhibited improved solubility in common solvents, which was beneficial for the preparation of membranes by the straightforward solution casting method. As shown in Fig. 2, both PTP and PTP-C*x* membranes were uniformly transparent. Among them, the PTP-C1 membrane exhibited a red brown color obviously due to the presence of iodine ions, while the other membranes PTP-C3 to PTP-C10 had a yellow color due to Br^-. Additionally, Fig. 2 also shows the surface SEM images of each membrane. It can be seen that all the membranes were uniform and dense without micropores, which was beneficial for fed gas separation in HT-PEMFCs.[6,8]

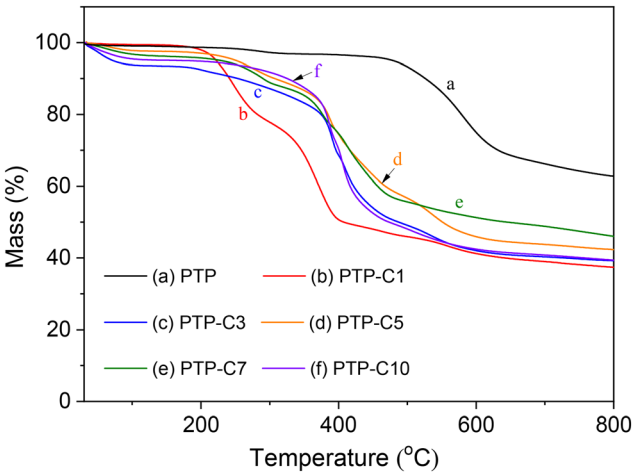

Fig. 3 TGA curves of (a) PTP and (b–f) PTP-C*x* membranes in a N_2 atmosphere at a heating rate of 10 °C min^{-1}.

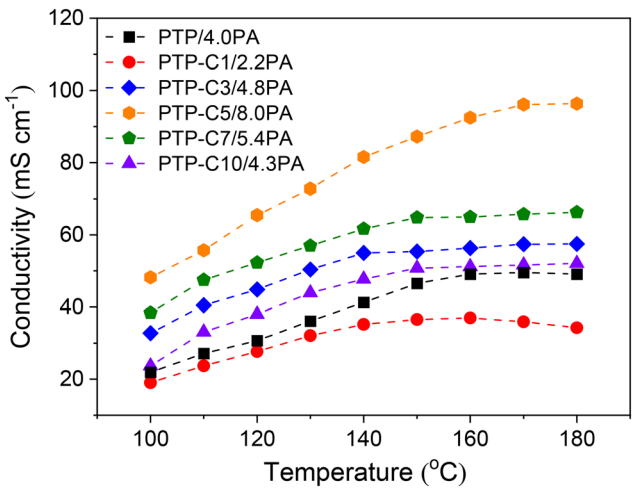

Fig. 4 Proton conductivities of the PTP and PTP-C*x* membranes doped in 85 wt% PA solution at 60 °C.

2.2 Thermal and chemical stabilities

Fig. 3 shows the TGA curves of PTP and PTP-C*x* in N_2. As previously reported,[27,30] the pure PTP polymer exhibited good thermal stability below 420 °C, which is also confirmed by our TGA result. As seen from Fig. 4, alkyl side chain grafting obviously decreased the thermal decomposition temperatures of the PTP-C*x* membranes. The weight loss below 100 °C was attributed to the loss of absorbed water.[31] As the temperature increased to 210 °C, the decomposition of alkyl side chains of the PTP-C*x* polymers occurred.[27,35,36] Above 420 °C, the weight loss mainly resulted from the degradation of the PTP main chain. Taking into account the thermal stability of PA, HT-PEMFCs are normally operated at temperatures ranging from 100 °C to 200 °C.[6,30] Hence, the PTP-C*x* membranes displayed a good thermal stability below 210 °C, which met the requirement for HT-PEMFCs.[5,8]

The chemical stability of a membrane is important for the long-term operation of fuel cells,[2,8] which is normally determined by Fenton tests in a solution consisting of 3.0% H_2O_2 and 4.0 ppm Fe^{2+} at 68 °C.[8,36] Fig. S1 (in the ESI†) shows the weight retention percentage of the PTP and PTP-C*x* membranes after a 48 h Fenton test. The inserted images show the appearance of the various membranes before and after the Fenton test. After treatment in Fenton's reagent for 48 h, the PTP membrane displayed a mass loss percentage of 9%, and it broke into pieces. Grafting alkyl side chains into the PTP membrane decreased the chemical stability of membranes. The weight loss of PTP-C1, PTP-C3 and PTP-C5 was 20%, 17% and 11%, respectively. As seen from the inserted images, the PTP-C1 membrane was broken into powder-like pieces, while PTP-C3 and PTP-C5 were broken into small pieces. As previously reported, QA-type group grafted membranes are normally unstable in Fenton solution.[31,36] Thus, the PTP-C*x* membranes displayed a more significant degradation than the PTP membrane during the Fenton test. The above results reveal that the chemical stability of either pure PTP or PTP-C*x* membranes needs to be improved in a future study.

2.3 Acid doping and swelling

The acid doping content of one HT-PEM not only illustrates the interaction between PA molecules and the membrane, but also directly affects the conductivity and mechanical stability.[5,9] Herein, in 85 wt% PA solution at 60 °C, the acid doping equilibrium of the membranes was determined. Table 1 summarizes the ADC%, ADL, *A*% and *V*% results of the PTP and various PTP-C*x* membranes. The presence of *N*-methylpiperidine groups in the repeating units of PTP made the membrane easily absorb PA through acid–base and hydrogen bonding interactions. Consequently, the ADC% and ADL of the PTP membrane reached around 120% and 4.0. Similarly, for the PTP-C*x* membranes, the attached alkyl groups had a great effect on the acid doping of the membranes. PTP-C1 with the methyl side chains exhibited a decreased ADC% of around 58% compared with PTP, indicating the poor PA absorption capacity of PTP-C1. With increasing length of alkyl side chains, both the ADC% and ADL of the membranes increased accordingly. The PTP-C5 membrane with pentyl side chains achieved the highest ADC% and ADL (*i.e.* 202% and 8.0) among all the investigated membranes. This may be because the grafted pentyl side chains provided more free volume for PA doping.[5,9,36,37] However, by further increasing the length of alkyl side chains, the PTP-C7 and PTP-C10 membranes displayed decreased ADC% values. This could be due to the significant steric hindrance of heptyl and decyl groups and their increased hydrophobic nature. Thus, choosing a suitable alkyl side chain is a crucial factor for superior PA doping.

In addition, the doped PA molecules would result in deformation of membranes due to the plasticization of PA molecules.[8,17,24] As depicted in Table 1, the PTP-C*x* membrane with a higher ADC% generally had a larger area and volume swellings. For example, the PTP-C5 membrane with the highest ADC% of 202% had the largest volume swelling of 66.2% among all the PTP-C*x* membranes. Nevertheless, the *V*% of PTP-C5 was comparable to that of PTP (*i.e.* 63.1%), although the former had a one and a half times higher ADC% than the latter. This results from the bigger free volume of PTP-C5 than that of PTP as previously reported.[36,38] Compared to HT-PEMs in other studies, the PTP-C5 membrane exhibited lower or similar volume swelling. For instance, blend membranes consisting of PEI and PEK-cardo exhibited an ADC% of 174% and a *V*% value of 120%.[21] The PTP-41% BeIm membrane with a methylene benzimidazole side chain displayed a *V*% of 148% with its ADC% being around 215%.[31] The P-83% APy membrane composed of 1-(3-aminopropyl)pyrrolidin-2-one (APy) and PEK-cardo showed an ADC% of 228% and a volume swelling of 98%.[46]

Table 1 ADC%, ADL and swellings of the PTP and PTP-C*x* membranes after doping in 85 wt% PA solution at 60 °C

Membrane	ADC%	ADL	*S*%	*V*%
PTP	120 ± 5	4.0 ± 0.2	36.0 ± 2	63.1 ± 5
PTP-C1	58 ± 3	2.2 ± 0.1	21.8 ± 1	33.5 ± 2
PTP-C3	126 ± 5	4.8 ± 0.2	33.7 ± 2	43.6 ± 3
PTP-C5	202 ± 8	8.0 ± 0.4	45.9 ± 3	66.2 ± 4
PTP-C7	131 ± 5	5.4 ± 0.3	40.1 ± 2	52.6 ± 5
PTP-C10	112 ± 5	4.3 ± 0.3	23.3 ± 1	41.0 ± 3

2.4 Proton conductivity and mechanical properties

Proton conductivities of the various PA doped PTP-C*x* membranes at 100–180 °C are summarized in Fig. 4. Generally, higher temperature can accelerate proton migration.[7,8] Thus, the conductivity of each membrane was correspondingly upgraded as the temperature increased. For instance, the conductivity of the PTP/4.0PA membrane raised from 21.9 mS cm^{-1} to 49.1 mS cm^{-1} when the temperature increased from 100 °C to 180 °C. Most importantly, Fig. 4 indicates that the proton conductivities of the membranes had a strong correlation with the pendant alkyl side chains. As shown in Table 1, the PTP-C*x* membranes with different side chains and grafting degrees exhibited different ADLs. Based on the widely investigated proton conduction mechanism of PA doped HT-PEMs,[8,9,39] the PA doping level is the main influencing factor for the proton conductivity. Compared with the PTP/4.0PA membrane, the PTP-C1/2.2PA membrane exhibited a lower conductivity at each temperature, obviously due to the lower ADL of PTP-C1 than that of PTP. Upon introducing longer alkyl side chains, the PTP-C*x* membranes achieved increased ADLs, resulting in higher conductivities compared with PTP/4.0PA. Among all the investigated membranes, the PTP-C5 membrane with the highest ADL of 8.0 possessed the highest conductivity of 96 mS cm^{-1} at 180 °C. Apparently, the high ADL of one HT-PEM benefits the formation of continuous hydrogen-bonding networks and transmission channels for fast proton migration.[5,16,39]

Additionally, PA molecules not only play a role in proton conduction, but also bring in plasticization and reduce the interaction between polymer chains.[8,26] Therefore, the trade-

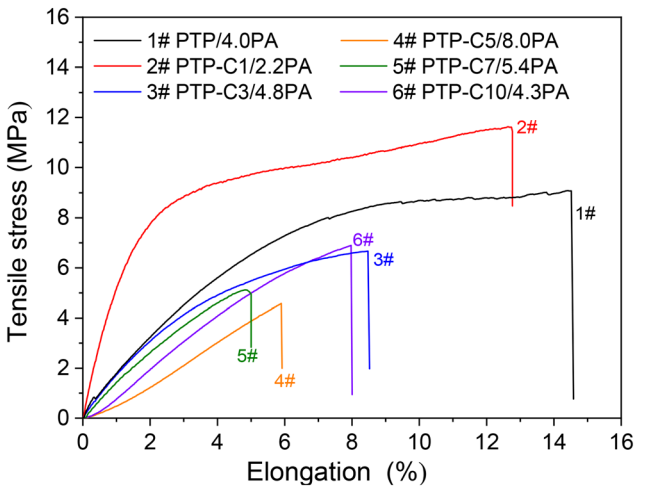

Fig. 5 Stress–strain curves of the PTP and PTP-C*x* membranes doped in 85 wt% PA solution at 60 °C.

off between mechanical stability and conductivity needs to be considered for the PA doped HT-PEMs. Fig. 5 depicts the mechanical stress–strain curves of the PTP-C*x*/PA membranes. It can be concluded that the chemical structure of alkyl side chains had a great effect on the tensile strength of PA doped membranes. The PA doped PTP-C1/2.2PA membrane displayed the highest tensile stress at break of 11.6 MPa, obviously resulting from its lowest ADL of 2.2. As the length of alkyl side chains increased, the PTP-C*x* membranes exhibited enhanced ADL and decreased tensile strength accordingly. As a result, the PTP-C5/8.0PA membrane exhibited the lowest tensile strength of 4.6 MPa at RT. Nevertheless, the PTP-C5/8.0PA membrane possessed comparable mechanical strength with those from recent studies. For instance, a grafted PTP membrane with an imidazolium ionic liquid (PTP-PMIM/323% PA) exhibited a tensile strength of 4.5 MPa,[34] while a blend membrane of PBI and poly(arylene ether) containing tetrazole biphenyl (PBI-TzPN25) with an ADC% of 440% exhibited a mechanical strength of around 5.8 MPa.[37] Benicewicz *et al.* reported that a PA doped membrane with a tensile strength of above 2 MPa could be assembled for testing HT-PEMFC performance,[40] illustrating that all PTP-C*x*/PA membranes in this study are promising candidates for fuel cell applications.

2.5 Fuel cell performance

Comprehensively considering the trade-off between tensile strength and conductivity, the PTP-C5/202% PA membrane was selected to assemble a MEA and measure the fuel cell performance under H_2 and air conditions without external humidification or backpressure. As shown in Fig. 6, the cell had high open circuit voltages (OCVs) of around 0.9 V at 160–210 °C, revealing the low gas permeability of PTP-C5/202% PA.[7,8] Meanwhile, the performance of the cell gradually improved with the increase of temperature, which resulted from the enhanced proton conductivity and faster electrode kinetics.[6] The cell displayed a peak power density of 316 mW cm^{-2} at 160 °C, which increased to 676 mW cm^{-2} at 210 ° C. However, the exact reason for this significantly high value at 210 °C is not clear so far, possibly resulting from the much higher electrode kinetics. Thus, more investigations on the characteristics of the MEA such as the HFR should be done to deeply understand this phenomenon in future work. Additionally, this value is high compared with those reported in other studies. For instance, a H_2–air cell with a crosslinked CrL-4.6% F_6PBI/13.5PA membrane displayed a peak power density of 360 mW cm^{-2} at 160 °C without backpressure,[11] while the peak power density of the cell based on the PTP/159.9% PA membrane was 387 mW cm^{-2} at 180 °C under H_2 and air conditions.[30] As widely reported, optimizing the operation conditions, electrode composition and MEA manufacturing will further increase the fuel cell performance.[5–7] In addition, replacing alkyl side chains with flexible *N*-oligo(ethylene glycol) (OEG) groups would further improve the membrane performance, as demonstrated by a PTP based AEM with terminal pendant OEG.[41] In short, the fuel cell results show that the PTP-C5/PA membrane has great potential in HT-PEMFC applications, also providing new options for other energy devices.[42,43]

3 Conclusions

In conclusion, a series of PA doped alkyl side chain substituted poly(terphenyl piperidinium) membranes have been synthesized for HT-PEMFCs. The presence of piperidinium cations endowed the membranes with PA doping capability, while the rigid wholly aromatic polymer chain maintained good dimensional and mechanical stabilities. The tailored pendant alkyl groups including methyl, propyl, pentyl, heptyl and decyl effectively adjusted the properties of the membranes. ^{1}H NMR spectra confirmed the successful synthesis of PTP and PTP-C*x* polymers. SEM images demonstrated that all the membranes were uniform and dense without micropores. Compared with PTP and methyl grafted PTP (PTP-C1) membranes, the other PTP-C*x* membranes with long alkyl side chains exhibited improved PA doping contents and conductivities. The optimized pentyl-substituted PTP

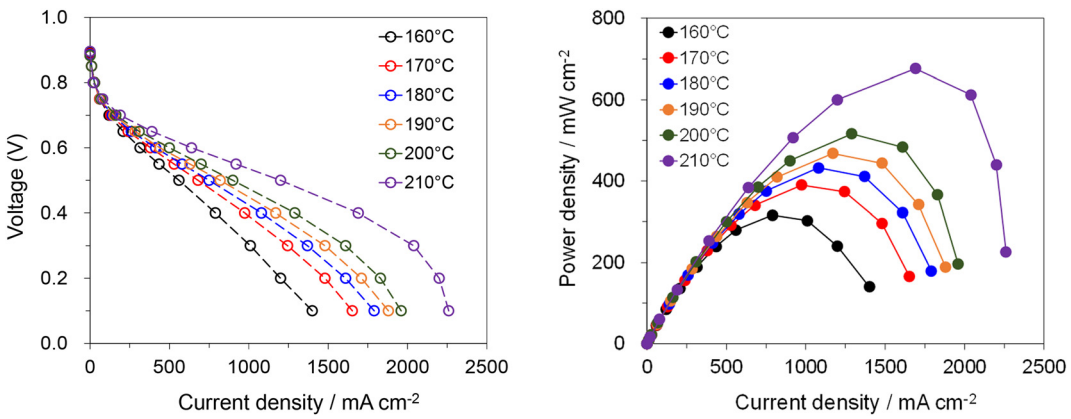

Fig. 6 Unhumidified H_2–air fuel cell performances of the cell assembled with the PTP-C5/202% PA membrane without backpressure at different temperatures. The Pt catalyst loading in both electrodes was 1.5 mg cm^{-2}.

membrane (PTP-C5) possessed the best overall performance. After immersing in 85 wt% PA at 60 °C, the PTP-C5 membrane achieved the highest PA doping content of 202% and reached the highest proton conductivity of 96 mS cm^{-1} at 180 °C. Meanwhile, this membrane also maintained a moderate tensile strength of 4.6 MPa at room temperature. A single cell equipped with the PTP-C5/PA membrane exhibited excellent fuel cell performances. The peak power density of the H_2–air HT-PEMFC reached 676 mW cm^{-2} at 210 °C without external humidification or backpressure. Thus, this work provides a simple design method for preparing advanced HT-PEMs.

4 Experimental

4.1 Synthesis of the PTP polymer

The PTP polymer was synthesized according to the reports of Guzman-Gutierrez *et al.*[44] and Jannasch *et al.*[27] The synthetic details were described in our previous studies.[31,33] The synthesized dark blue viscous mixture was added into 1 M $NaHCO_3$ aqueous solution to precipitate the polymer. The excess acid in the polymer was washed away using 1 M KOH solution, followed by washing with deionized water to neutrality and drying at 100 °C. A light yellow fiber like polymer was finally obtained.

4.2 Preparation of the PTP-C*x* membranes

Fig. 7 shows that quaternized PTP polymers with alkyl side chains of different lengths were synthesized through the Menshutkin reaction between PTP and various haloalkanes, including iodomethane (C1), 1-bromopropane (C3), 1-bromopentane (C5), 1-bromoheptane (C7) and 1-bromodecane (C10). Firstly, the haloalkane was separately dripped into a mixed solution of dimethyl sulfoxide (DMSO)/*N*-methyl-2-pyrrolidinone (NMP) with a volume ratio of 1 : 3. Then, PTP was added into the above mixture with the molar ratio of PTP to haloalkane being 1 : 1.5. After reacting at 80 °C for 16 h, the uniform orange solution was cooled to room temperature (RT) and then slowly poured into anhydrous ether, followed by washing three times to finally obtain the flexible side-chain alkyl grafted polymer PTP-C*x*, where *x* means the number of carbon atoms in the alkyl side chain.

The membranes were manufactured by a simple one-step solution casting method, as described below. Under the conditions of heating at 80 °C and magnetic stirring, each PTP-C*x* polymer was dissolved in DMSO to form a 2.5 wt% solution. The resulting solution was cast on a Petri dish, followed by evaporation of the solvent at 80 °C for 12 h. The resulting membrane was peeled off, followed by washing thoroughly in deionized water and drying in an oven at 80 °C for 12 h. Finally, a homogeneous membrane with a thicknesses of 40 ± 5 μm was prepared. In order to improve the solubility of PTP in DMSO, one drop of trifluoroacetic anhydride (TFA) was added into the PTP and DMSO mixture, and a TFA partially protonated PTP membrane was prepared accordingly.

4.3 Acid doping and swelling

The PA absorption of various films was determined by immersing the dry films in 85 wt% PA solution at 60 °C for

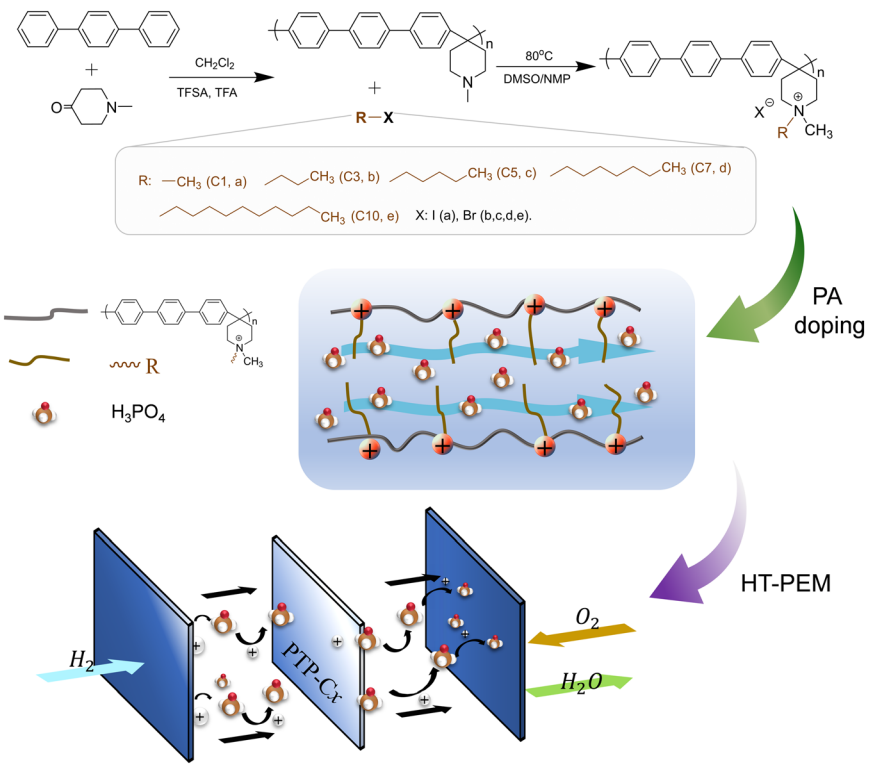

Fig. 7 Synthesis of PTP and fabrication of PTP-C*x* membranes.

72 h for the sake of measuring the amount of doped acid and swelling, as described previously.[25,26] After gently wiping PA off the surface of the membranes, the membranes were placed in a vacuum oven at 100 °C to remove free water, and then immediately weighed. The PA absorption capability of the membrane was expressed as the acid doping level (ADL), which is defined as the number of adsorbed PA molecules per polymer repeat unit as depicted in eqn (1). Meanwhile, the acid doping content (ADC) was also calculated in the present work and is defined as the mass ratio of PA molecules to the membrane according to eqn (2). The area and volume swellings (S% and V%) of each membrane were determined according to eqn (3) and (4).

$$\mathrm{ADL} = \frac{(m_{\mathrm{PA}} - m_{\mathrm{dry}})}{m_{\mathrm{dry}}} \times \frac{M_{\mathrm{polymer}}}{98} \quad (1)$$

$$\mathrm{ADC\%} = \frac{(m_{\mathrm{PA}} - m_{\mathrm{dry}})}{m_{\mathrm{dry}}} \times 100\% \quad (2)$$

$$S\% = \frac{S_1 - S_0}{S_0} \times 100\% \quad (3)$$

$$V\% = \frac{V_1 - V_0}{V_0} \times 100\% \quad (4)$$

where m_{PA} and m_{dry} mean the mass of the PA doped membrane and pure membrane, respectively. M_{polymer} represents the average molecular weight of the polymer repeat units of PTP and PTP-Cx. S and V represent the area and volume of each membrane before (0) and after (1) PA absorption.

4.4 Characterization

The inherent viscosity (η) was measured with an Ubbelohde viscometer at 25 °C in NMP using a polymer concentration of 100 mg dL^{-1}. Then, η was calculated according to eqn (5),[45] where t_s is the efflux time of the polymer solution, t_b is the outflow time of pure NMP, and c is the concentration.

$$\eta = \ln\left(\frac{t_s}{t_b}\right)/c \quad (5)$$

The chemical structures of various samples were characterized by ^{1}H NMR. The physicochemical properties were determined in terms of scanning electron microscopy (SEM), thermogravimetric analysis (TGA), Fenton tests, tensile stress–strain curves and conductivity as previously reported.[26,31]

The fuel cell performance of the membrane electrode assembly (MEA) was determined on a home-made fuel cell setup. The Pt/C catalyst and PBI binder loadings were 1.5 mg cm^{-2} and 0.07 mg cm^{-2} respectively in the electrodes, which were obtained as previously reported.[21,46] H_2 was supplied at a rate of 80 mL min^{-1}, and air was supplied at a rate of 200 mL min^{-1}. The polarization curves of the H_2–air fuel cell were determined from 160 °C to 210 °C without any humidification and backpressure.

Conflicts of interest

The authors declare no conflict of interest.

Acknowledgements

We gratefully acknowledge the Natural Science Foundation of China (51603031) and the Fundamental Research Funds for the Central Universities of China (N2005026). Special thanks to Prof. Qingfeng Li at the Technical University of Denmark (DTU) for helping to test the single cell performance.

References

1 B. G. Pollet, S. S. Kocha and I. Staffell, Current status of automotive fuel cells for sustainable transport, *Curr. Opin. Electrochem.*, 2019, **16**, 90–95.
2 Y. Wang, Z. Yang, L. Wu, L. Ge and T. Xu, Ion exchange membrane "ABC" – A key material for upgrading process industries, *Chin. J. Chem.*, 2021, **39**, 825–837.
3 F. Xu, Y. Chen, J. Li, Y. Han, B. Lin and J. Ding, Robust poly(alkyl-fluorene isatin) proton exchange membranes grafted with pendant sulfonate groups for proton exchange membrane fuel cells, *J. Membr. Sci.*, 2022, **664**, 121045.
4 Y. Chen, F. Xu, J. Li, Y. Han, J. Qiao, J. Liu, Y. Xu and B. Lin, Poly(fluorenyl terphenyl piperidinium) with sulfonated side chains for the application of high-temperature proton exchange membranes, *ACS Appl. Energy Mater.*, 2023, **6**, 2594–2601.
5 V. Atanasov, A. S. Lee, E. J. Park, S. Maury, E. D. Bac, C. Fujimoto, M. Hibbs, I. Matanovic, J. Kerres and Y. S. Kim, Synergistically integrated phosphonated poly(pentafluorostyrene) for fuel cells, *Nat. Mater.*, 2020, **20**, 370–377.
6 D. Aili, D. Henkensmeier, S. Martin, B. Singh, Y. Hu, J. O. Jensen, L. N. Cleemann and Q. Li, Polybenzimidazole-based high-temperature polymer electrolyte membrane fuel cells: New insights and recent progress, *Electrochem. Energy Rev.*, 2020, **3**, 793–845.
7 R. Haider, Y. Wen, Z. Ma, D. Wilkinson, L. Zhang, X. Yuan, S. Song and J. Zhang, High temperature proton exchange membrane fuel cells: Progress in advanced materials and key technologies, *Chem. Soc. Rev.*, 2021, **50**, 1138–1187.
8 Q. Li, J. O. Jensen, R. F. Savinell and N. J. Bjerrum, High temperature proton exchange membranes based on polybenzimidazoles for fuel cells, *Prog. Polym. Sci.*, 2009, **34**, 449–477.
9 D. Aili, J. S. Yang, K. Jankova, D. Henkensmeier and Q. Li, From polybenzimidazoles to polybenzimidazoliums and polybenzimidazolides, *J. Mater. Chem. A*, 2020, **8**, 12854–12886.
10 J. S. Wainright, J.-T. Wang, D. Weng, R. F. Savinell and M. Litt, Acid-doped polybenzimidazoles: A new polymer electrolyte, *J. Electrochem. Soc.*, 1995, **142**, 121–123.
11 J. Yang, Q. Li, L. N. Cleemann, J. O. Jensen, C. Pan, N. J. Bjerrum and R. He, Crosslinked hexafluoropropylidene polybenzimidazole membranes with chloromethyl

polysulfone for fuel cell applications, *Adv. Energy Mater.*, 2013, **3**, 622–630.

12 J. W. Peng, S. C. Wang, X. Z. Fu, J. L. Luo, L. Wang and X. J. Peng, Achieving over 1,000 mW cm−2 power density based on locally high-density cross-linked polybenzimidazole membrane containing pillar [5] arene bearing multiple alkyl bromide as a cross-linker, *Adv. Funct. Mater.*, 2022, 2212464.

13 F. Liu, S. Wang, H. Chen, J. Li, X. Wang, T. Mao and Z. Wang, The impact of poly (ionic liquid) on the phosphoric acid stability of polybenzimidazole-base HT-PEMs, *Renewable Energy*, 2021, **163**, 1692–1700.

14 H. Guo, Z. Li, H. Pei, P. Sun, L. Zhang, P. Li and X. Yin, Stable branched polybenzimidazole high temperature proton exchange membrane: Crosslinking and pentaphosphonic-acid doping lower fuel permeability and enhanced proton transport, *J. Membr. Sci.*, 2022, **644**, 120092.

15 X. F. Hao, Z. Li, M. Xiao, Z. H. Huang, D. M. Han, S. Huang, W. Liu, S. J. Wang and Y. Z. Meng, Intermolecular acid-base-pairs containing poly (p-terphenyl-co-isatin piperidinium) for high temperature proton exchange membrane fuel cells, *Energy Environ. Mater.*, 2023, e12621.

16 M. Georgezi, C. L. Chochos, N. Gourdoupi, S. G. Neophytides and J. K. Kallitsis, High performance polymer electrolytes based on main and side chain pyridine aromatic polyethers for high and medium temperature proton exchange membrane fuel cells, *J. Power Sources*, 2011, **196**, 9382–9390.

17 K. J. Kallitsis, R. Nannou, A. K. Andreopoulouа, M. K. Daletou, D. Papaioannou, S. G. Neophytides and J. K. Kallitsis, Crosslinked wholly aromatic polyether membranes based on quinoline derivatives and their application in high temperature polymer electrolyte membrane fuel cells, *J. Power Sources*, 2018, **379**, 144–154.

18 Z. Guo, R. Xiu, S. Lu, X. Xu, S. Yang and Y. Xiang, Submicro-pore containing poly (ether sulfones) poly vinyl pyrrolidone membranes for high temperature fuel cell applications, *J. Mater. Chem. A*, 2015, **3**, 8847–8854.

19 X. Ren, H. Li, K. Liu, H. Lu, J. Yang and R. He, Preparation and investigation of reinforced PVP blend membranes for high temperature polymer electrolyte membranes, *Fibers Polym.*, 2018, **19**, 2449–2457.

20 W. Zhao, X. Xu, H. Bai, J. Zhang, S. Lu and Y. Xiang, Self-crosslinked polyethyleneimine-polysulfone membrane for high temperature proton exchange membrane, *Acta Chim. Sin.*, 2020, **78**, 69–75.

21 Y. Jin, R. Liu, X. Che, T. Wang and J. Yang, New high temperature polymer electrolyte membranes based on poly (ethylene imine) crosslinked poly (ether ketone cardo), *J. Electrochem. Soc.*, 2021, **168**, 054524.

22 E. Cetina-Mancilla, L. I. Olvera, J. Balmaseda, M. Forster, F. A. Ruiz-Treviño, J. Cárdenas, E. Vivaldo-Lima and M. G. Zolotukhin, Well-defined, linear, wholly aromatic polymers with controlled content and position of pyridine moieties in macromolecules from one-pot, room temperature, metal-free step-polymerizations, *Polym. Chem.*, 2020, **11**, 6194.

23 M. Carta, R. Malpass-Evans, M. Croad, Y. Rogan, J. C. Jansen, P. Bernardo, F. Bazzarelli and N. B. McKeown, An efficient polymer molecular sieve for membrane gas separations, *Science*, 2013, **339**, 303–307.

24 Y. Jin, T. Wang, X. Che, J. Dong, Q. Li and J. Yang, Poly (arylene pyridine)s: New alternative materials for high temperature polymer electrolyte fuel cells, *J. Power Sources*, 2022, **526**, 231131.

25 Y. Jin, T. Wang, W. Tang, N. Yu and J. Yang, High-performance poly (biphenyl acetylpyridine) and poly (ether ketone cardo) blend membranes for high-temperature polymer electrolyte membrane fuel cells, *Macromol. Mater. Eng.*, 2022, **307**, 2200300.

26 T. Wang, Y. Jin, T. Mu, T. Wang and J. Yang, Troger's base polymer blended with poly (ether ketone cardo) for high temperature proton exchange membrane fuel cell applications, *J. Membr. Sci.*, 2022, **654**, 120539.

27 J. Olsson, T. Pham and P. Jannasch, Poly (arylene piperidinium) hydroxide ion exchange membranes: Synthesis, alkaline stability, and conductivity, *Adv. Funct. Mater.*, 2018, **28**, 1702758.

28 J. Wang, Y. Zhao, B. P. Setzler, S. Rojas-Carbonell, C. B. Yehuda, A. Amel, M. Page, L. Wang, K. D. Hu, L. Shi, S. Gottesfeld, B. J. Xu and Y. S. Yan, Poly (aryl piperidinium) membranes and ionomers for hydroxide exchange membrane fuel cells, *Nat. Energy*, 2019, **4**, 392–398.

29 H. Peng, Q. Li, M. Hu, L. Xiao, J. Lu and L. Zhuang, Alkaline polymer electrolyte fuel cells stably working at 80 °C, *J. Power Sources*, 2018, **390**, 165–167.

30 H. J. Bai, H. Q. Peng, Y. Xiang, J. Zhang, H. N. Wang, S. F. Lu and L. Zhuang, Poly (arylene piperidine)s with phosphoric acid doping as high temperature polymer electrolyte membrane for durable, high-performance fuel cells, *J. Power Sources*, 2019, **443**, 227219.

31 Y. P. Jin, T. Wang, X. F. Che, J. H. Dong, R. H. Liu and J. S. Yang, New high-performance bulky N-heterocyclic group functionalized poly (terphenyl piperidinium) membranes for HT-PEMFC applications, *J. Membr. Sci.*, 2022, **641**, 119884.

32 W. Tang, T. Mu, X. Che, J. Dong and J. Yang, Highly selective anion exchange membrane based on quaternized poly (triphenyl piperidine) for the vanadium redox flow battery, *ACS Sustainable Chem. Eng.*, 2021, **9**, 14297.

33 X. Che, W. Tang, J. Dong, D. Aili and J. Yang, Anion exchange membranes based on long side-chain quaternary ammonium-functionalized poly (arylene piperidinium)s for vanadium redox flow batteries, *Sci. China Mater.*, 2022, **65**, 683.

34 Y. Jin, X. Che, Y. Xu, J. Dong, C. Pan, D. Aili, Q. Li and J. Yang, An imidazolium type ionic liquid functionalized ether-free poly (terphenyl piperidinium) membrane for high temperature polymer electrolyte membrane fuel cell applications, *J. Electrochem. Soc.*, 2022, **169**, 024504.

35 S. Maity, A. Sannigrahi, S. Ghosh and T. Jana, N-alkyl polybenzimidazole: Effect of alkyl chain length, *Eur. Polym. J.*, 2013, **49**, 2280–2292.

36 J. Yang, J. Wang, C. Liu, L. Gao, Y. Xu, Q. Che and R. He, Influences of the structure of imidazolium pendants

on the properties of polysulfone-based high temperature proton conducting membranes, *J. Membr. Sci.*, 2015, **493**, 80–87.

37 N. N. Krishnan, N. M. H. Duong, A. Konovalova, J. H. Jang, H. S. Park, H. J. Kim, A. Roznowska, A. Michalak and D. Henkensmeier, Polybenzimidazole/ tetrazole-modified poly (arylene ether) blend membranes for high temperature proton exchange membrane fuel cells, *J. Membr. Sci.*, 2020, **614**, 118494.

38 D. Tian, T. Gu, S. N. Yellamilli and C. Bae, Phosphoric acid-doped ion-paircoordinated PEMs with broad relative humidity tolerance, *Energies*, 2020, **13**, 1924.

39 L. Vilciauskas, M. E. Tuckerman, G. Bester, S. J. Paddison and K. D. Kreuer, The mechanism of proton conduction in phosphoric acid, *Nat. Chem.*, 2012, **4**, 461–466.

40 L. Xiao, H. Zhang, E. Scanlon, L. S. Ramanathan, E.-W. Choe, D. Rogers, T. Apple and B. C. Benicewicz, High-temperature polybenzimidazole fuel cell membranes via a sol-gel process, *Chem. Mater.*, 2005, **17**, 5328–5333.

41 L. Liu, L. Bai, Z. Liu, S. Miao, J. Pan, L. Shen, Y. Shi and N. Li, Side-chain structural engineering on poly(terphenyl piperidinium) anion exchange membrane for water electrolysers, *J. Membr. Sci.*, 2023, **665**, 121135.

42 X.-R. Yun, Y.-F. Chen, P.-T. Xiao and C.-M. Zheng, Review on oxygen-free vanadium-based cathodes for aqueous zinc-ion batteries, *J. Electrochem.*, 2022, **28**, 2219004.

43 W.-F. Xie and M.-F. Shao, Water electrolysis for efficient hydrogen production, *J. Electrochem.*, 2022, **28**, 2214008.

44 M. T. Guzman-Gutierrez, D. R. Nieto, S. Fomine, S. L. Morales, M. G. Zolotukhin, M. C. G. Hernandez, H. Kricheldorf and E. S. Wilks, Dramatic enhancement of superacid-catalyzed polyhydroxyalkylation reactions, *Macromolecules*, 2011, **44**, 194–202.

45 J. Dong, N. Yu, X. Che, R. Liu, D. Aili and J. Yang, Cationic ether-free poly(bis-alkylimidazolium) ionene blend polybenzimidazole as anion exchange membranes, *Polym. Chem.*, 2020, **11**, 6037–6046.

46 R. Liu, J. Wang, X. Che, T. Wang, D. Aili, Q. Li and J. Yang, Facile synthesis and properties of poly (ether ketone cardo)s bearing heterocycle groups for high temperature polymer electrolyte membrane fuel cells, *J. Membr. Sci.*, 2021, **636**, 119584.